

Electrochemical Potential-Step Investigations of the Aerobic Interconversions of [NiFe]-Hydrogenase from *Allochromatium vinosum*: Insights into the Puzzling Difference between Unready and Ready Oxidized Inactive States

Sophie E. Lamle,[†] Simon P. J. Albracht,[‡] and Fraser A. Armstrong^{*†}

Contribution from the Department of Chemistry, Inorganic Chemistry Laboratory, Oxford University, South Parks Road, Oxford, OX1 3QR, England, and Swammerdam Institute for Life Sciences, Biochemistry, University of Amsterdam, Plantage Muidergracht 12, NL-1018 TV Amsterdam, The Netherlands

Received April 9, 2004; E-mail: fraser.armstrong@chem.ox.ac.uk

Abstract: Dynamic electrochemical studies, incorporating catalytic voltammetry and detailed potential-step manipulations, provide compelling evidence that the oxidized inactive state of [NiFe]-hydrogenases termed Unready (or Ni-A) contains a product of partial reduction of O₂ that is trapped in the active site.

Introduction

The biological hydrogen cycle is attracting considerable interest, not only because of its fundamental importance in microbiology and biochemistry, but also in regard to the technological implications of understanding the properties of the enzymes that are involved. Hydrogenases are found both in prokaryotes and in eukaryotes,^{1–3} where they catalyze the interconversion between H₂ and protons, as shown in eq 1:



There are two main classes of hydrogenase: [FeFe]-hydrogenases, in which Fe is the only metal at the active site, and [NiFe]-hydrogenases, which contain a Ni and an Fe atom at the active site. In this paper, we describe novel electrochemical kinetic experiments on the prototypical [NiFe]-hydrogenase from *Allochromatium vinosum*. [NiFe]-hydrogenases consist of a large subunit (60 kDa) containing the [NiFe] active site and a small subunit (30 kDa) containing at least one [4Fe–4S] cluster. The crystal structure of the hydrogenase from *Desulfovibrio gigas*,^{4,5} which contains the same prosthetic groups as the *A. vinosum* enzyme, shows that the small subunit houses a series of three Fe–S centers – a [4Fe–4S] cluster closest to the [NiFe] site and called the “proximal” cluster, a “medial” [3Fe–4S] cluster, and a [4Fe–4S] cluster close to the protein surface called the “distal” cluster. These clusters act as a “wire” to transfer

electrons to and from the buried active site, as well as a reservoir able to store up to three electrons. The medial cluster has a much higher reduction potential (ca. –30 mV) than the distal and proximal clusters (ca. –300 mV).⁶ Hydrogen molecules are believed to enter or leave the active site through a “gas channel” that is revealed crystallographically by the binding of Xe atoms (when the crystal is placed under high-pressure xenon) and by molecular dynamics calculations.⁷ The active site, shown in Figure 1, contains unusual small ligands coordinated at the Fe atom: these have been identified as one CO and two CN[–].^{5,8–12} Four cysteine sulfurs are coordinated, two bridging between the Ni and Fe atoms and two as terminal ligands to the Ni atom. Figure 1 shows that an additional bridging ligand of variable nature (thus represented as “X”) is also present in some states of the enzyme. The nature of this ligand as it exists in inactive states is addressed in this paper.

The various states of the [NiFe]-center are distinguished by spectroscopic methods, notably EPR and FTIR¹² (see Scheme 1). At least three redox states are proposed to be directly involved in catalysis: these are called Ni_a–S (or Ni–SI), Ni_a–C*, and Ni_a–SR.^{1,13–15} The two most oxidized states called

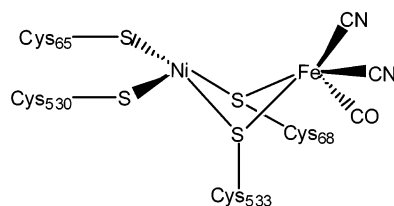
[†] Oxford University.

[‡] University of Amsterdam.

- (1) Cammack, R.; Frey, M.; Robson, R., Eds. *Hydrogen as a Fuel: Learning from Nature*; Taylor and Francis: London and New York, 2001.
- (2) Vignais, P. M.; Billoud, B.; Meyer, J. *FEMS Microbiol. Rev.* **2001**, *25*, 455–501.
- (3) Adams, M. W. W.; Stiefel, E. I. *Science* **1998**, *282*, 1842.
- (4) Volbeda, A.; Charon, M. H.; Piras, C.; Hatchikian, E. C.; Frey, M.; Fontecilla-Camps, J. C. *Nature* **1995**, *373*, 580–587.
- (5) Volbeda, A.; Garcia, E.; Piras, C.; De Lacey, A. L.; Fernández, V. M.; Hatchikian, E. C.; Frey, M.; Fontecilla-Camps, J. C. *J. Am. Chem. Soc.* **1996**, *118*, 12989–12996.

- (6) Pershad, H. R.; Duff, J. L. C.; Heering, H. A.; Duin, E. C.; Albracht, S. P. J.; Armstrong, F. A. *Biochemistry* **1999**, *38*, 8992–8999.
- (7) Montet, Y.; Amara, P.; Volbeda, A.; Vernede, X.; Hatchikian, E. C.; Field, M. J.; Frey, M.; Fontecilla-Camps, J. C. *Nat. Struct. Biol.* **1997**, *4*, 523–526.
- (8) Bagley, K. A.; Van Garderen, C. J.; Chen, M.; Duin, E. C.; Albracht, S. P. J.; Woodruff, W. H. *Biochemistry* **1994**, *33*, 9229–9236.
- (9) Bagley, K. A.; Duin, E. C.; Roseboom, W.; Albracht, S. P. J.; Woodruff, W. H. *Biochemistry* **1995**, *34*, 5527–5535.
- (10) De Lacey, A. L.; Hatchikian, E. C.; Volbeda, A.; Frey, M.; Fontecilla-Camps, J. C.; Fernández, V. M. *J. Am. Chem. Soc.* **1997**, *119*, 7181–7189.
- (11) Happe, R. P.; Roseboom, W.; Pierik, A. J.; Albracht, S. P. J.; Bagley, K. A. *Nature* **1997**, *385*, 126–126.
- (12) Happe, R. P.; Roseboom, W.; Albracht, S. P. J. *Eur. J. Biochem.* **1999**, *259*, 602–608.
- (13) Maroney, M. J.; Bryngelson, P. A. *J. Biol. Inorg. Chem.* **2001**, *6*, 453–459.
- (14) Fan, H. J.; Hall, M. B. *J. Biol. Inorg. Chem.* **2001**, *6*, 467–473.
- (15) De Lacey, A. L.; Fernández, V. M.; Rousset, M.; Cavazza, C.; Hatchikian, E. C. *J. Biol. Inorg. Chem.* **2003**, *8*, 129–134.

Active



Inactive

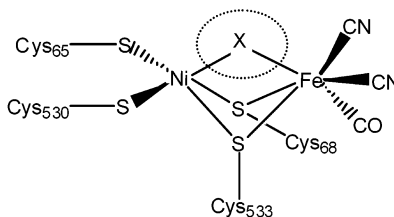
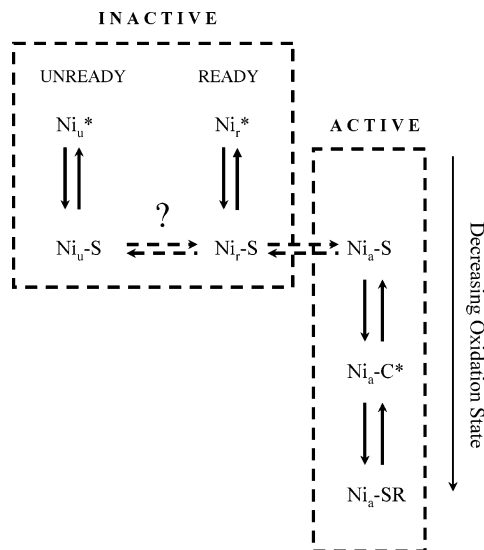


Figure 1. Structures of the catalytic center of [NiFe]-hydrogenases as summarized from existing crystallographic data. Inactive states contain an extra ligand (X) in a bridging position between the Ni and Fe atoms.

Scheme 1. Simplified Overview of the Spectroscopically Characterized States of the Ni–Fe Active Site of [NiFe]-Hydrogenases (those states marked with an * are EPR detectable)



“Unready” (variously Ni_u^* or Ni–A) and “Ready” (variously Ni_r^* or Ni–B) are inactive and need to be activated by reduction.¹⁶ (The asterisk indicates that the state is EPR-detectable.) Aerobically purified enzyme from *A. vinosum* contains a mixture of the Ready and Unready states, and it is noted that the Ready state activates rapidly upon contact with H_2 , whereas activation of the Unready state by incubation with H_2 takes hours. Throughout this Article, we will use the terms Ready and Unready because they emphasize the kinetic distinction that we are addressing. The oxidation levels of the enzyme are defined also by the oxidation states of the three Fe–S clusters, which are included by adding the shorthand notation contained in brackets (o = oxidized, r = reduced, for clusters listed in the order proximal, medial, distal). Thus, $Ni_r^*(oro)$ refers to the Ready state in which the medial cluster is reduced and the proximal and distal clusters are oxidized. For the *A.*

vinosum enzyme, procedures have been developed to oxidize samples so that either the Ready or the Unready state is formed preferentially.¹⁷ The best method of preparing the Ready state is to dilute H_2 -reduced enzyme at pH 9 into O_2 -saturated buffer: this produces 95% in the Ready state. A good way to prepare Unready is to take H_2 -reduced enzyme at pH 6, replace the H_2 with CO, and slowly admit O_2 .

In the presence of redox mediators, the Unready and Ready states can be converted in one-electron reactions to their respective reduced states Ni_u-S (Ni–SU) and Ni_r-S (Ni–SI), both of which are EPR-silent and catalytically inactive but distinguished on the basis of their IR bands that arise from the CO and CN^- ligands. Reduction of Unready to Ni_u-S is reversible, although above 30 °C, Ni_u-S converts slowly to the inactive Ni_r-S state which converts further to the active states Ni_a-S , Ni_a-C^* , and Ni_a-SR .¹⁸ The EPR-detectable Ni_a-C^* state is believed to have a hydride ligand bound to the Ni–Fe site in a bridging position.^{10,19–21}

From previous crystallographic studies, the main structural difference between active and inactive states, represented in Figure 1, appears to be the presence of an additional ligand between the Ni and Fe atoms.^{5,22,23} However, the *D. gigas* enzyme used to obtain crystals for those studies was a mixture of several states: EPR analysis of the crystals showed 50% of Ni sites to be EPR-silent, while of the remaining half, 85% was Ni_u^* (Unready) and 15% was Ni_r^* (Ready).⁴ The EPR-silent enzyme molecules were not in an active or Ni_r-S state, because development of full H_2 -uptake activity required hours of incubation under H_2 . Enzyme thus prepared was mainly in the Ni_u^* or Ni_u-S states. When reduced *A. vinosum* hydrogenase in $H_2^{16}O$ was oxidized by $^{17}O_2$ to produce mixtures of Ni_u^* and Ni_r^* , the EPR spectra of either product displayed line broadening due to a magnetic interaction between Ni(III) and a nearby ^{17}O nucleus.²⁴ The bridging ligand detected in the crystal structure was therefore suggested to be oxygenic. An OH^- ligand was proposed and has since remained the favored candidate, certainly in either of the oxidized inactive states Ni_u^* and Ni_r^* .

However, the specific structural differences between the Ready and Unready states that account for their contrasting rates of activation have not been resolved.^{4,5,17,22,25–28} Recent studies by Carepo et al.,²⁸ in which reduced enzyme in $H_2^{17}O$ was reoxidized by $^{16}O_2$, indicated that the Unready state of the *D.*

(16) Fernández, V. M.; Hatchikian, E. C.; Patil, D. S.; Cammack, R. *Biochim. Biophys. Acta* **1986**, 883, 145–154.

- (17) Bleijlevens, B.; Faber, B. W.; Albracht, S. P. J. *J. Biol. Inorg. Chem.* **2001**, 6, 763–769.
 (18) Coremans, J.; Van der Zwaan, J. W.; Albracht, S. P. J. *Biochim. Biophys. Acta* **1992**, 1119, 157–168.
 (19) Niu, S.; Thomson, L. M.; Hall, M. B. *J. Am. Chem. Soc.* **1999**, 121, 4000–4007.
 (20) Brecht, M.; van Gastel, M.; Buhrke, T.; Friedrich, B.; Lubitz, W. *J. Am. Chem. Soc.* **2003**, 125, 13075–13083.
 (21) Van der Zwaan, J. W.; Albracht, S. P. J.; Fontijn, R. D.; Slater, E. C. *FEBS Lett.* **1985**, 179, 271–277.
 (22) Stadler, C.; De Lacey, A. L.; Montet, Y.; Volbeda, A.; Fontecilla-Camps, J. C.; Conesa, J. C.; Fernández, V. M. *Inorg. Chem.* **2002**, 41, 4424–4434.
 (23) Volbeda, A.; Montet, Y.; Vernede, X.; Hatchikian, E. C.; Fontecilla-Camps, J. C. *Int. J. Hydrogen Energy* **2002**, 27, 1449–1461.
 (24) Van der Zwaan, J. W.; Coremans, J. M. C. C.; Bouwens, E. C. M.; Albracht, S. P. J. *Biochim. Biophys. Acta* **1990**, 101–110.
 (25) De Lacey, A.; Pardo, A.; Fernández, V. M.; Dementin, S.; Adryanczyk-Perrier, G.; Hatchikian, E. C.; Roussel, M. *J. Biol. Inorg. Chem.* **2004**, 9, 636–642.
 (26) Garcin, E.; Vernede, X.; Hatchikian, C.; Volbeda, A.; Frey, M.; Fontecilla-Camps, J. C. *Structure* **1999**, 7, 557–566.
 (27) Armstrong, F. A. *Curr. Opin. Chem. Biol.* **2004**, 8, 133–140.
 (28) Carepo, M.; Tierney, D. L.; Brondino, C. D.; Yang, T. C.; Pamplona, A.; Telsler, J.; Moura, I.; Moura, J. J. G.; Hoffman, B. M. *J. Am. Chem. Soc.* **2002**, 124, 281–286.

gigas enzyme contains an oxygen species derived from the solvent. Work by Bleijlevens et al.¹⁷ showed that a specific proton hyperfine splitting was present in the Ni_I^* state, but not in the Ni_U^* state. It was further suggested that in the Ni_I^* state a hydroxo group might be terminally bound to Ni, whereas in the Ni_U^* state it is bridging between the Ni and Fe atoms. Another suggestion, based on density functional calculations, is that Ready and Unready both contain a bridging hydroxide, but differ in the position of a nearby carboxyl group that can form a hydrogen bond to one of the terminal cysteine-S atoms coordinated to the Ni.²² These structural differences could conceivably present a sufficiently large barrier to account for the dramatic differences in activation kinetics for the two species. However, these proposals also suggest that Unready and Ready should interconvert, but no firm evidence for this has been reported.

The conventional way to measure H_2 oxidation activity is to monitor reduction of a redox dye such as a viologen.^{1,29} However, for investigating an enzyme as complex as a hydrogenase, this approach represents a rather blunt tool. The technique used in this paper, protein film voltammetry (PFV), which is the dynamic electrochemistry of protein molecules confined to an electrode surface, allows detailed studies of the catalytic action of a minuscule sample of redox enzymes as a direct and variable function of the electrode potential.^{30,31} Provided electron transfer with the electrode is fast, the electrochemical measurements reflect the intrinsic chemistry of the enzyme. Importantly, the catalytic current is directly related to the catalytic rate in a particular direction (negative = reduction; positive = oxidation). Thus, the rate of change of current is the rate of change of catalytic rate, that is, the rate of the activation or inactivation. The electrode coated with enzyme can be transferred between different solutions, such as buffers at different pH. Moreover, dissolved gases can be varied easily, simply by exchanging the gas in the headspace of an enclosed electrochemical cell.

Investigations of *A. vinosum* [NiFe]-hydrogenase adsorbed on a rotating disk pyrolytic graphite "edge" (PGE) electrode have shown that the active site oxidizes H_2 at a rate that is comparable to an adsorbed Pt catalyst, as used in commercial fuel cells.^{6,32,33} The opportunities to study fundamental properties of the active site were obvious, and recent studies focused on the anaerobic electro-oxidation reaction and the reductive reactivation of the product, which was assigned as the Ready state.³⁴ In this investigation, we address the nature and properties of the Ready and Unready states that are formed when [NiFe]-hydrogenase is exposed to O_2 . The problem is of physiological relevance because many organisms that produce hydrogenases (such as *Allochromatium vinosum*) also utilize O_2 in their life cycles. The question then is how the organisms manage to avoid or minimize the loss of hydrogenase activity when O_2 is present. The experiments probe the quantitative requirements for formation of Unready under different conditions of turnover and

electron availability and provide important information on the kinetics of its reactivation.

Materials and Methods

The [NiFe]-hydrogenase from *A. vinosum* (*Av*) was prepared as described previously.¹⁸ All experiments were carried out in a glovebox (M. Braun) under an anaerobic N_2 atmosphere ($\text{O}_2 < 2$ ppm). The rotating disk pyrolytic graphite "edge" (PGE) electrode was constructed as described previously³⁵ and was used in conjunction with an EG&G M636 electrode rotator. All electrodes were polished with a 1 μm alumina slurry (Buehler) and sonicated thoroughly before each experiment. A three-electrode system was used in conjunction with an all-glass electrochemical cell that was equipped with an "o"-ring gasket: this gasket gave a snug fit around the electrode rotator, sealing the internal headspace of the electrochemical cell from the glovebox atmosphere.³⁴ This design allowed gases to be introduced quickly and reliably at a constant pressure through inlet and outlet sidearms, and less than 5 min was required to achieve complete equilibration with the cell solution (typically 3 mL) when the electrode was rotated, with the cell temperature at 45 °C. The counter electrode was a piece of platinum wire, and the reference was a saturated calomel electrode (SCE) situated in a Luggin sidearm filled with 0.1 M NaCl. The main cell compartment was jacketed and thermostated at the required temperature, while the reference electrode sidearm was well separated and kept at a constant temperature (a nonisothermal configuration). The reference potential was corrected with respect to the standard hydrogen electrode (SHE) by using $E_{\text{SHE}} = E_{\text{SCE}} + 242$ mV at 25 °C.³⁶ All values given in this Article have been adjusted to conform to the SHE scale.

Linear sweep/cyclic voltammetry and chronoamperometry were performed using an Autolab PGSTAT 20 or PGSTAT 30 electrochemical analyzer (Eco Chemie, The Netherlands) controlled by GPES software (Eco Chemie, The Netherlands) and equipped with a digital staircase scan generator and an electrochemical detection unit (ECD) for increased sensitivity. Voltammograms were recorded in digital mode, with the fractional sampling duration (α) = 0.5. Tests carried out without enzyme on the electrode showed no currents due to H_2 oxidation or proton reduction over the range of at least 400 to -650 mV. Chronoamperometric experiments were carried out by sampling the current every second following the potential step (duration of step $\ll 1$ s).

A mixed buffer system was used in all experiments. This consisted of 15 mM in each of sodium acetate, MES (2-[*N'*-morpholino]ethanesulfonic acid), HEPES (*N'*-[2-hydroxyethyl]-piperazine-*N'*-2-ethanesulfonic acid), TAPS (*N'*-tris[hydroxymethyl]-methyl-3-amino-propanesulfonic acid), and CHES (2-[*N'*-cyclohexylamino]ethanesulfonic acid), each purchased from Sigma, with 0.1 M NaCl as supporting electrolyte. All solutions were prepared using purified water (Millipore: 18 M Ω cm) and titrated with NaOH or HCl to the desired pH at the experimental temperature. A coadsorbate, polymyxin B sulfate (from a stock solution), was added to all cell solutions (final concentrations of 200 $\mu\text{g mL}^{-1}$) to stabilize the protein film. After each experiment, a sample of the cell solution was taken, and the pH was checked at the appropriate temperature. The gases N_2 and H_2 were obtained from Air Products, and CO was obtained from BOC. Stock solutions of O_2 -saturated buffer were prepared by taking a portion of the pH-adjusted buffer, placing it in a suba-sealed vial, and bubbling pure O_2 through it for 3 min. Concentrations of O_2 were estimated by assuming that the concentration in the stock solution injected into the cell was that expected for equilibrium with 1 bar at room temperature, that is, approximately 1 mM at 45 °C.³⁷

After polishing and sonicating the PGE electrode before each experiment, a film of hydrogenase was prepared by placing the electrode

(29) Cammack, R.; Williams, R.; Guigliarelli, B.; More, C.; Bertrand, P. *Biochem. Soc. Trans.* **1994**, *22*, 721–725.

(30) Armstrong, F. A.; Heering, H. A.; Hirst, J. *Chem. Soc. Rev.* **1997**, *26*, 169–179.

(31) Léger, C.; Elliott, S. J.; Hoke, K. R.; Jeuken, L. J. C.; Jones, A. K.; Armstrong, F. A. *Biochemistry* **2003**, *42*, 8653–8662.

(32) Jones, A. K.; Sillery, E.; Albracht, S. P. J.; Armstrong, F. A. *Chem. Commun.* **2002**, 866–867.

(33) Léger, C.; Jones, A. K.; Roseboom, W.; Albracht, S. P. J.; Armstrong, F. A. *Biochemistry* **2002**, *41*, 15736–15746.

(34) Jones, A. K.; Lamle, S. E.; Pershad, H. R.; Vincent, K. A.; Albracht, S. P. J.; Armstrong, F. A. *J. Am. Chem. Soc.* **2003**, *125*, 8505–8514.

(35) Sucheta, A.; Cammack, R.; Weiner, J.; Armstrong, F. A. *Biochemistry* **1993**, *32*, 5455–5465.

(36) Bard, A. J.; Faulkner, L. R. *Electrochemical Methods: Fundamentals and Approaches*; Wiley: New York, 2001.

(37) Lide, R. D. *CRC Handb. Chem. Phys.* **1996–1997**, 77.

in a dilute solution of the enzyme (0.1–1.0 μM hydrogenase, pH 6.0 or 7.0, 45 $^{\circ}\text{C}$, containing 20 mg/mL polymyxin B sulfate) under N_2 . The electrode potential was cycled between -558 and $+242$ mV versus SHE at 10 mV s^{-1} until a stable catalytic response was obtained, as described previously.⁶ The electrode was either rotated at 300 rpm (which generally gave a slightly improved coverage, and only proton reduction was monitored) or held stationary (which allowed the progress of adsorption to be monitored also through the intense peak produced by reoxidation of the H_2 formed by enzymatic proton reduction and remaining at the electrode). This typically required 20 min. The enzyme solution was then removed from the cell and replaced with fresh buffer (typically 3 mL) to avoid problems arising from exchange of enzyme between electrode and bulk solution. As a precaution, the electrode with the enzyme film was then held at -550 mV under H_2 at 45 $^{\circ}\text{C}$ for 30 min, to ensure the whole sample was in the active form.³⁸

When H_2 is first introduced into the cell, the electrode exhibits diffusion-controlled H_2 oxidation.^{6,32,33} This causes a problem when trying to monitor subtle changes in enzyme activity (diffusion control masks the details of the catalytic properties of the enzyme).³⁴ Therefore, the electrode was “polished” gently with a piece of damp cotton wool to remove some of the enzyme from the surface. This ensures that the catalytic current is independent of the electrode rotation rate within a large range (1500–2500 rpm). Most experiments were carried out at pH 6.0 because anaerobic inactivation is slower and the enzyme film is more stable than at higher pH.^{34,39}

Results

Figure 2A shows a chronoamperometry experiment to compare the rate of inactivation produced by injection of O_2 (i) with that induced by applying an oxidizing potential under anaerobic conditions (ii). In both cases, the enzyme-coated PGE electrode was rotated at 2500 rpm in a cell containing pH 6.1 buffer at 45 $^{\circ}\text{C}$, and the current was monitored at a potential of 242 mV. In the former case, 1 mL of O_2 -saturated buffer was injected into 3 mL of electrolyte (thus the final concentration of O_2 is approximately 0.3 mM).

The effect of O_2 is profound: the reaction is very rapid in comparison to anaerobic inactivation, in good agreement with recent stopped-flow FTIR experiments carried out under more stoichiometric conditions which show that reaction is complete within a fraction of a second.⁴⁰ Figure 2B shows a cyclic voltammogram recorded with a rotating electrode at a slow scan rate (1.2 mV s^{-1}) at pH 6.3 under 1 bar H_2 . While the potential was scanned from -558 to 242 mV, 1 mL of O_2 -saturated buffer was injected into the cell (at approximately -50 mV) and rapid inactivation was observed, as for Figure 2A. While the potential continued to climb, O_2 was removed from the cell solution by the flow of H_2 ; then on the return sweep, more than 80% of the H_2 oxidation activity was recovered rapidly in a peak-like response. The shape of the peak and the potential at which reactivation occurs (the position of maximum slope, determined from the derivative di/dE where current = i and potential = E , termed E_{switch} : see annotation in Figure 2B) are very similar to the result obtained when the enzyme has been inactivated anaerobically, that is, using an oxidizing potential alone (see later for more details). The results therefore suggested that under these conditions, inactivation by O_2 produces mainly the Ready state.

The final O_2 concentration (in the cell) was varied to establish its effect on the extent and rate of inactivation. In practice,

(38) Albracht, S. P. J. *Biochim. Biophys. Acta* **1994**, *1188*, 167–204.

(39) Jones, A. K. D. *Philos. Thesis*, University of Oxford, 2002.

(40) George, S. J.; Kurkin, S.; Thorneley, R. N. F.; Albracht, S. P. J. *Biochemistry* **2004**, *43*, 6808–6819.

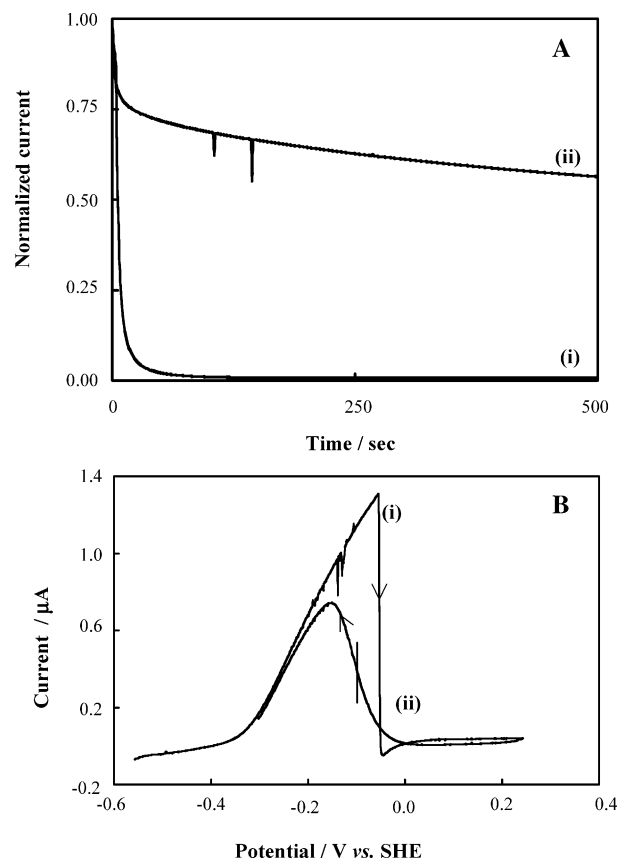


Figure 2. (A) Chronoamperometric experiment comparing anaerobic and aerobic inactivation of [NiFe]-hydrogenase. (i) Experiment carried out under 1 bar H_2 , 242 mV with 1 mL of O_2 -saturated buffer added to the electrochemical cell at the start of the measurement (final concentration 0.3 mM O_2). (ii) Experiment carried out under 1 bar H_2 at a potential of 242 mV with no addition of O_2 . Other experimental conditions are identical: pH 6.1, 45 $^{\circ}\text{C}$, electrode rotation rate 2500 rpm. (B) Slow cyclic voltammogram (1.2 mV s^{-1}) measured at pH 6.3 with a rotation rate of 2500 rpm under 1 bar H_2 . The cycle starts at -558 mV, and at (i) 1 mL of O_2 -saturated buffer is injected. H_2 is then flushed through the headspace to remove excess O_2 . At (ii), reductive activation commences: the recovery of activity is quantified by a potential value, E_{switch} , marked by the vertical line, which is the position of maximum slope given by the derivative di/dE . The arrows indicate the direction of cycling.

complete inactivation was obtained provided the O_2 concentration was above approximately $0.4 \mu\text{M}$. Most experiments were therefore carried out using a quantity of O_2 -saturated buffer (0.1 mL corresponding, after dilution, to a maximum concentration of approximately $30 \mu\text{M}$ O_2) that was sufficient to ensure complete reaction without much excess O_2 .

For more precise measurements of the time-potential characteristics of the transformations, we used chronoamperometry, with which we could generate various sequences of gas changes and potential steps and monitor the enzyme's response in each case. Figure 3 shows an experiment carried out at 45 $^{\circ}\text{C}$ under H_2 , for which the time course (X -axis) is labeled with the potential steps and other operations performed at each stage. Because it may help clarify the experiment, we have added a “route map” that portrays the sequence of operations in the potential domain. It is thus easy to see how the enzyme can be manipulated with respect to the thermodynamic potential for the redox couple $2\text{H}^+/\text{H}_2$ (approximately -0.37 V at pH 6.0, 45 $^{\circ}\text{C}$) and the potential that defines the enzyme's active–inactive interconversions (E_{switch}): indeed, the ability to control

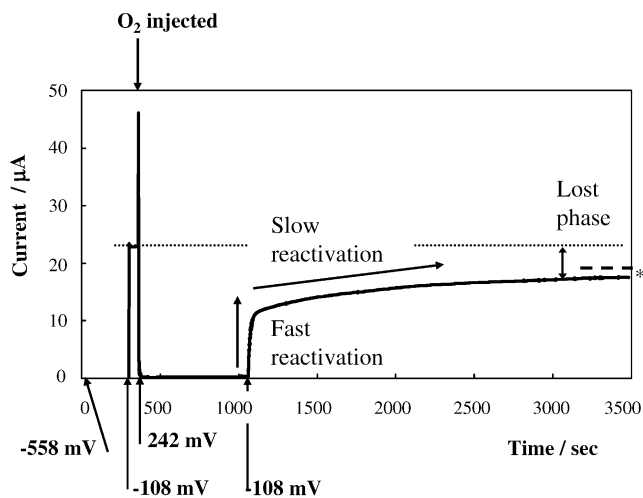


Figure 3. Current versus time trace for a chronoamperometry experiment in which [NiFe]-hydrogenase adsorbed on a PGE electrode is subjected to a sequence of potential steps under an atmosphere of H_2 (1 bar). The lower diagram shows a “route map” of the potential-step sequence with operations carried out at particular times and electrode potentials. The time spent at each stage is given. The potential was initially held at -558 mV for 300 s under 1 bar H_2 before the potential was stepped to -108 mV for 60 s. A step was then made to 242 mV (a potential at which O_2 is not reduced) at which point 0.10 mL of O_2 -saturated buffer was injected. The headspace was then flushed with H_2 (1 bar) for 600 s to remove O_2 from the solution, after which the potential was stepped back to -108 mV to initiate reductive activation. Other experimental conditions were: pH 6.0, 45°C , and electrode rotation rate 2500 rpm. The dashed line shows the level to which the current was expected to return if the enzyme had not been subjected to O_2 , as gauged from control experiments. The dotted line (spanning the entire time course) corresponds to the maximum current that should have returned (the same as that measured at 300 s). The small difference is indicated by *.

the direction and rate of electron flow in the enzyme is a crucial feature of these experiments. The potential was initially held at -558 mV for 300 s, judged to be sufficient time for the headgas to equilibrate with the cell solution, and then the potential was stepped to -108 mV for 60 s followed by a step to 242 mV. At -108 mV, no inactivation occurs without O_2 (this is used as an activity reference), while at 242 mV, the enzyme inactivates slowly in the absence of O_2 . At 242 mV, 0.10 mL of O_2 -saturated buffer was injected into the cell, resulting in rapid loss of activity. The headspace was then flushed with H_2 for 600 s to remove the residual O_2 from the solution, while the potential was held constant at 242 mV to prevent reductive reactivation. The potential was then stepped back to -108 mV, and reductive reactivation was observed. Two phases are observable in the reactivation trace, one fast and one slow.

As we propose later in this paper, the fast and slow phases correspond to the activation of Ready and Unready states, respectively. The slow phase is first order with a rate constant $0.0025 \pm 0.0004 \text{ s}^{-1}$; in other words, the half-life of the Unready

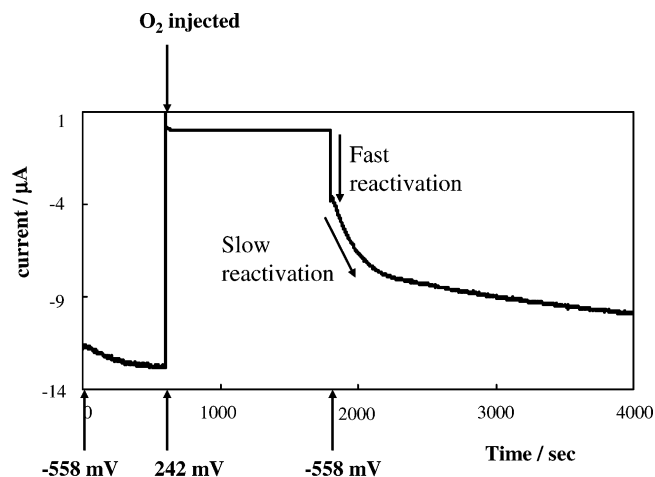


Figure 4. Current versus time trace for a chronoamperometry experiment carried out under 1 bar N_2 . Initially the potential was held at -558 mV with N_2 flowing through the headspace, before being stepped to 242 mV at which point 0.1 mL of O_2 -saturated buffer was injected. The potential was held at 242 mV for 1200 s to ensure all O_2 was removed from solution before the potential was stepped back to -558 mV to initiate reductive activation. Other experimental conditions: pH 6.0, 45°C , and electrode rotation rate 2500 rpm. The route map is shown below.

state is approximately 5 min at 45°C . The final current was always lower than observed initially, reflecting both slow loss of enzyme molecules from the electrode over the extended course of the experiment and loss due to other kinds of inactivation. Shown also in Figure 3 is the final current (dashed line) measured in a control experiment that recorded the loss in activity when the same manipulations were carried out without O_2 . Superoxide is known to destroy Fe–S clusters⁴¹ and might be produced either at the electrode (although precautions were taken to avoid excessively negative potentials when injecting O_2) or by reaction of O_2 at the reduced distal cluster (O_2 now serving as a remote one-electron acceptor). These observations were not pursued further in this study, but they suggest that the ratio of slow to fast phase will always be a slight underestimate.

A similar experiment (Figure 4) was carried out under N_2 to observe the activation process as it appears when monitoring proton reduction instead of H_2 oxidation. Initially, the potential was held at -558 mV for 600 s before being stepped to 242 mV, and then 0.10 mL of O_2 -saturated buffer was injected. The headspace was flushed with N_2 to remove residual O_2 before the potential was stepped back down to -558 mV, and the activation process was monitored, this time as a reduction current. As before, much of the activity is regained immediately

(41) Gardner, P.; Fridovich, I. *J. Biol. Chem.* **1991**, *266*, 1478–1483.

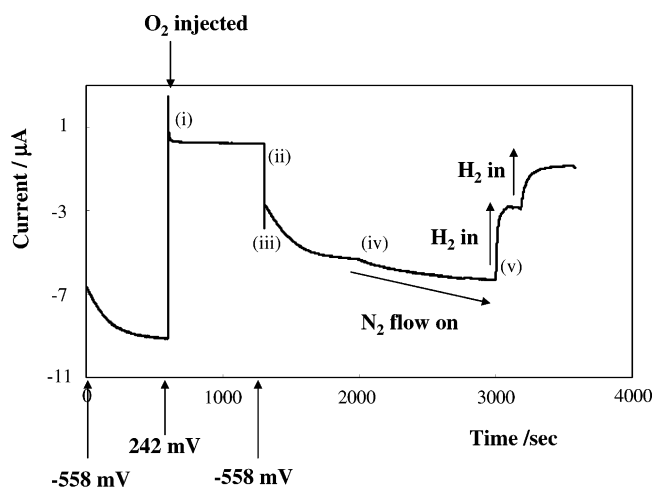


Figure 5. Current versus time trace for a chronoamperometric experiment carried out to examine the effect of N_2 and H_2 on proton reduction activity during reactivation of the enzyme. Initially the potential was held at -558 mV under N_2 flow for 600 s. At (i), the potential was stepped to 242 mV and 0.10 mL of O_2 -saturated buffer was injected into the cell. The potential was held at 242 mV for 600 s while N_2 was passed through the headspace to remove the remaining O_2 . The N_2 flow was then turned off, and the potential was stepped back to -558 mV (ii) to reactivate the enzyme. At 2000 s, the N_2 flow was restored (iv), and then at 3000 s, N_2 was turned off and H_2 was introduced into the cell in two bursts (v). Other experimental conditions were pH 6.0, $45^\circ C$, electrode rotation rate 2500 rpm.

in a fast phase (this is faster than observed in Figure 3, because for the Ready state the rate of activation depends strongly on the potential even below E_{switch}). However, the slow phase is more complex than when measuring H_2 oxidation activity, and this was investigated further, the issue being that proton reduction by [NiFe]-hydrogenase is known to be inhibited by the H_2 that is produced.³³

Figure 5 shows how the proton reduction activity is affected by exchanging N_2 and H_2 in the headspace. Initially, the potential was held at -558 mV for 600 s under a flow of N_2 . The potential was then stepped to 242 mV, and at (i) 0.1 mL of O_2 -saturated buffer was injected into the cell and the potential was held constant while the residual O_2 was flushed from the solution. The N_2 flow was then stopped, and the potential was stepped back to -558 mV at which reductive activation was observed. The initial fast phase (ii) is now followed by a slower phase (iii) before the current levels off. At 2000 s, the flow of N_2 was switched on again (iv), and a further increase in current was observed, resulting not in a plateau but remaining as a residual slope. At 3000 s, H_2 was allowed to flow into the headspace for a few seconds (v), which caused a large and instantaneous attenuation of proton reduction activity. Introduction of more H_2 caused further loss in proton reduction activity, and finally the current reached a steady low level. The proton reduction current is extremely sensitive to inhibition by the H_2 product,³³ so it is difficult to study the slow phase of reactivation in this way. Similar results were obtained if Ar was used as headgas instead of N_2 .

Figure 6 shows the reactivation traces obtained after injecting O_2 at various different potentials and gas conditions: 242 and 42 mV under N_2 , and 217 and 42 mV under H_2 . All experiments were carried out in pH 6.0 buffer at $45^\circ C$, with the electrode rotating at 2500 rpm. They show clearly that a larger fraction of fast-phase species is formed when O_2 is injected at a more negative potential and under H_2 . Following this lead, an exten-

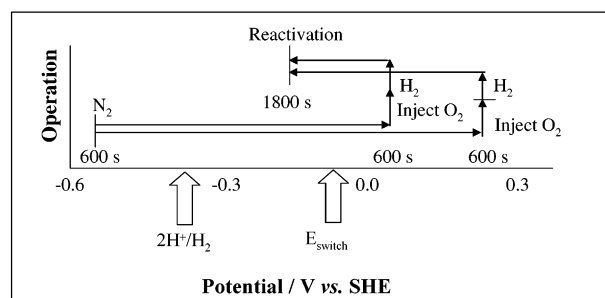
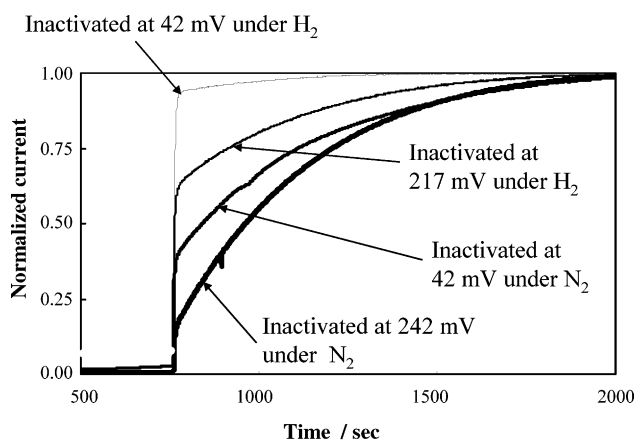


Figure 6. Current versus time traces for chronoamperometric experiments to examine the percentage of slow phase formed at different potentials under a N_2 or H_2 atmosphere (1 bar in either case). Initially the potential was held at -558 mV for 600 s before being stepped to the potentials indicated. Next, 0.10 mL of O_2 -saturated buffer was injected into the cell, and the gas was changed from N_2 to H_2 to remove the remaining O_2 before the potential was stepped back to -158 mV. Other experimental conditions: pH 6.0, $45^\circ C$, and electrode rotation rate 2500 rpm. The route map, generalized to cover variations in conditions, is shown below.

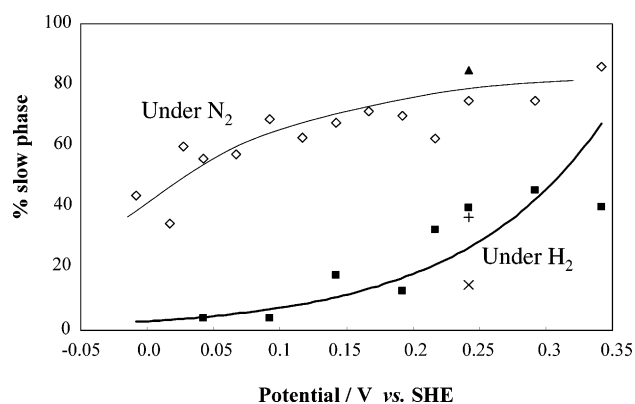


Figure 7. Plot showing the percentage of slow phase formed under N_2 (\diamond) or H_2 (\blacksquare) as a function of the electrode potential applied while O_2 is injected. \blacktriangle is for an experiment where the potential was held at -258 mV for 300 s under N_2 before being stepped to 242 mV. The data points \times and $+$ are for experiments carried out at pH 8.8, under H_2 and N_2 , respectively.

sive series of experiments was carried out in which O_2 was injected at different potentials, under atmospheres of either 1 bar H_2 or 1 bar N_2 ; the fractions of slow phase obtained in each case are shown in Figure 7. The lines shown are curve fits to depict the trends and are not based on any mathematical model.

We varied the time gap between stepping the potential to the desired value and injecting O_2 , the reasoning being that enzyme molecules might not equilibrate immediately with the electrode potential. There was no significant difference between

time periods of 0 (i.e., immediate injection), 3, and 6 s. However, an experiment under N_2 in which the potential sequence included an intermediate step for 300 s to a potential of -258 mV before a potential step to 242 mV and O_2 injection produced an increase in the fraction of slow phase. At -258 mV, the enzyme is able to oxidize H_2 (remaining in the cell or in the enzyme molecule itself as a product of proton reduction), but the potential is still well below E_{switch} so there is no anaerobic inactivation. These data are included in Figure 7. Data from two experiments carried out in pH 8.8 are also included in Figure 7: they show a decrease in the amount of slow phase formed under both H_2 and N_2 , as compared to inactivation at pH 6.0. In another experiment, designed to generate the maximum amount of Unready state, the potential was initially held at -558 mV under H_2 before stepping the potential to a value below E_{switch} and introducing CO into the headspace, which caused immediate and complete loss of H_2 oxidation activity. The headgas was then changed to N_2 , and after the solution was purged for 10 min to remove CO the potential was stepped to 242 mV, at which stage O_2 was injected. After the solution was purged with N_2 for a further 10 min to remove O_2 , the potential was stepped down to -158 mV to reactivate the enzyme. The result showed a small increase in the fraction of slow phase, similar to that observed for the experiment described above in which the potential was held at a value below E_{switch} and under N_2 before the O_2 injection.

It was now necessary to examine whether there is a difference in the potential at which the enzyme is reactivated (E_{switch}) when more than 80% of the enzyme is in the Unready state. Figure 8A shows an experiment in which the Unready state was generated by injecting O_2 under N_2 at 242 mV, pH 6.0; then after flushing with H_2 exactly as described above, the potential was scanned very slowly (at 0.3 mV s^{-1}) in the negative direction. (Note that the cycle shown in Figure 2B was carried out at pH 6.3, and at a higher scan rate, i.e., 1.2 mV s^{-1} .) As compared to the result obtained (Figure 8B) when starting from >95% Ready (generated by injecting O_2 at -8 mV under 1 bar H_2 and then following the same procedure as described above), the shape is much more rounded, and there is a small negative shift in E_{switch} . Analogous experiments were conducted at pH 8.8, and the results are also shown.

Figure 9 shows experiments to investigate how the rate of activation depends on the electrode potential (driving force) that is applied, when H_2 oxidation is monitored. These experiments followed up the results shown in Figures 4 and 5 which suggested that the slow phase is little accelerated at very low potential (as instead observed through H^+ reduction, which is inhibited by H_2). After incubating the hydrogenase film for 1 h under H_2 at 45 °C, while holding the potential at -558 mV, the potential was stepped to 242 mV and held there for 60 s. Next, 0.25 mL of O_2 -saturated buffer was injected into the cell and H_2 was flushed through the headspace for 600 s. Finally, the potential was stepped in the negative direction to reactivate the enzyme. Figure 9A and B compares current–time traces following reactivation potentials of -108 and -208 mV, respectively. Figure 9C shows semilog plots of $\log(|i_{lim} - i_t|)$ versus time for experiments carried out with reactivation potentials at decreasing values below E_{switch} , that is, -108 , -158 , -208 , and -308 mV. Remarkably, even over the large range of driving forces used (all potentials are below E_{switch}),

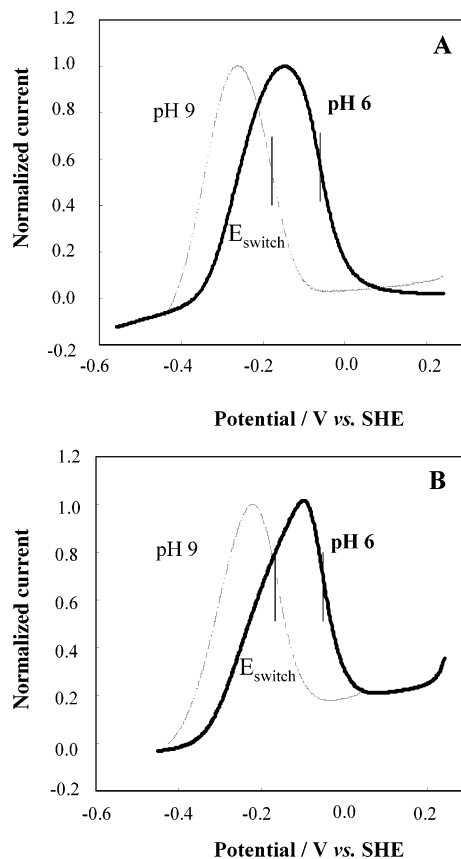


Figure 8. Voltammograms showing reactivation of [NiFe]-hydrogenase inactivated under conditions favoring the Unready (A) or Ready (B) states. For (A), the enzyme film was preposited at 242 mV under N_2 and inactivated with 0.10 mL of saturated O_2 buffer. H_2 was then passed through the headspace for 600 s to flush out O_2 before the voltammogram was recorded, from 242 to -558 mV at 0.3 mV s^{-1} . For (B), the enzyme film was preposited at -8 mV under H_2 and inactivated with 0.10 mL of saturated O_2 buffer, and then the same procedure was followed as for (A). Other experimental conditions: pH 6.0, 45 °C, and electrode rotation rate 2500 rpm. (A) and (B) show also the same experiments carried out at pH 8.8: note the large negative shift in E_{switch} in either case.

the rates show no significant dependence on potential. This is in marked contrast to reactivation of the Ready state, the rate of which is highly potential dependent even below E_{switch} ,³⁴ as is apparent just when comparing the appearance of the fast phases in Figure 9A and B.⁴²

Experiments were carried out to determine how the rate of reactivation and the proportion of slow phase depend on pH. Figure 10A shows the current–time trace for an experiment carried out under H_2 at pH 7.0, in which O_2 -saturated buffer (0.1 mL) was injected at 242 mV and the headspace was flushed with H_2 before the potential was stepped to -233 mV to reactivate the enzyme. Figure 10B shows the same experiment carried out at pH 8.8. The lower total extent of recovered activity at pH 8.8 reflects the greater instability of the enzyme film at higher pH, as reported earlier.³⁹ Figure 10C shows the corresponding semilog plots ($\log(|i_{lim} - i_t|)$ versus time) for the experiments conducted at pH 6.0, 7.0, and 8.8. In all cases, rate constants are cleanly first order and identical among themselves and as calculated from Figure 9C. The lower fraction of slow phase produced at higher pH (20% at pH 8.8 vs 40% at pH

(42) As expected, at higher potentials, the rate and extent of activation decrease. A full investigation of the potential dependence is currently in progress.

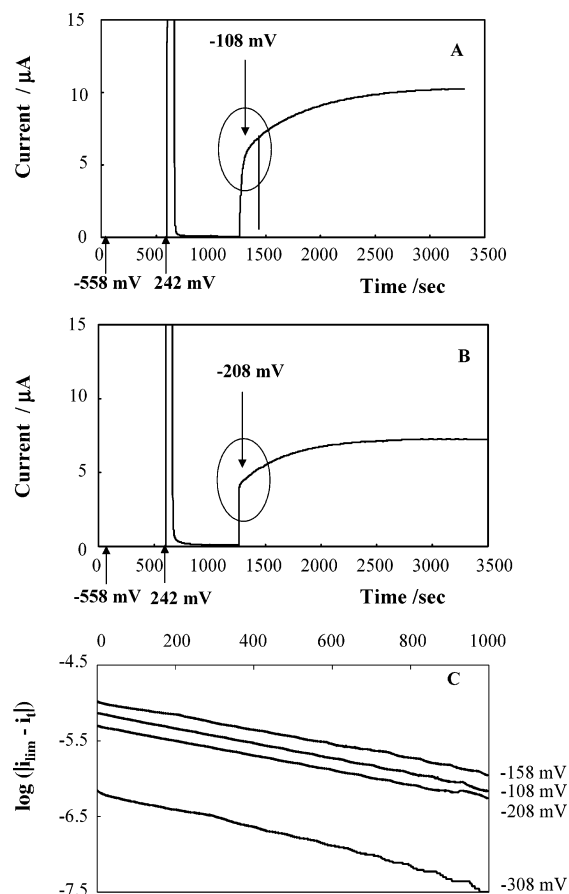


Figure 9. Results of chronoamperometry experiments to examine the potential dependence of the rate of reductive activation. The electrode potential was initially held at -558 mV for 600 s under an atmosphere of 1 bar H_2 , and then stepped to 242 mV for 60 s at which stage 0.25 mL of O_2 -saturated buffer was injected. H_2 was immediately flushed through the headspace for 600 s to remove O_2 before the potential was stepped back to initiate reductive reactivation. Panels A and B show the results obtained for reactivation potentials of -108 and -208 mV, respectively. (C) Semilog kinetic plots generated from the slow reactivation phase observable in panels A and B along with data from other experiments carried out with different reactivation potentials. Other experimental conditions: pH 6.0, 45 °C, and electrode rotation rate 2500 rpm. The basic route map, apart from reactivation potentials, is the same as that for Figure 3.

6.0) prompted a further experiment in which the enzyme was inactivated under 1 bar N_2 instead of H_2 . In this case, the same procedure was followed as described for Figure 5A, and injection of O_2 was made at 242 mV. Once again, the fraction of slow phase was lower at pH 8.8 (40%) than observed at pH 6.0 (80%).

The temperature dependence of the rate constant (k) for the slow phase was measured to obtain the activation parameters. Experiments were carried out over the temperature range 25–50 °C, at pH 6.0. Kinetic traces were obtained after injecting O_2 -saturated buffer at 242 mV under H_2 , and then stepping the potential to -158 mV after flushing the headspace for 10 min. (Below 25 °C, the rate of the slow phase becomes too slow to give reliable results, due to competing slow loss of enzyme from the electrode surface.) The rate constants are shown in Table 1. Figure 11 shows that a plot of $\log(k/T)$ versus $1/T$ is linear, yielding $\Delta H^\ddagger = 84.2 \pm 0.7$ kJ mol $^{-1}$ and $\Delta S^\ddagger = -28 + 5$ J K $^{-1}$ mol $^{-1}$.

Experiments were also carried out in D_2O instead of H_2O to determine whether there is an isotope effect on the rate of the

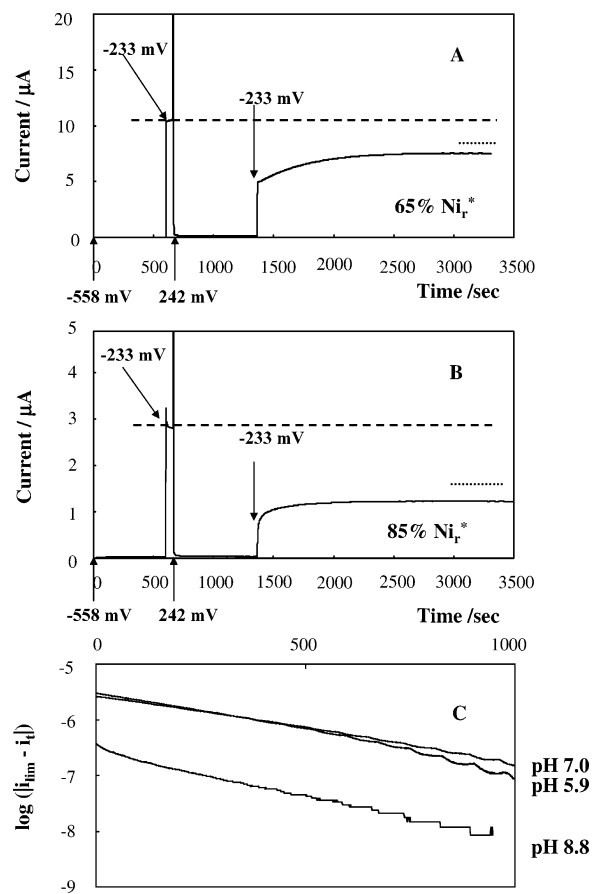


Figure 10. Results of chronoamperometry experiments to examine the pH dependence of reductive activation. Initially the potential was held at -558 mV for 600 s before being stepped to -233 mV for 60 s. The potential was then stepped to 242 mV, and 250 μ L of O_2 -saturated buffer was injected into the cell. H_2 (1 bar) was immediately flushed through the headspace for 600 s to remove O_2 before the potential was stepped back to -233 mV to initiate reactivation. Panels A and B show the results obtained at pH 7.0 and pH 8.8, respectively. Panel C shows the corresponding semilog kinetic plots generated from the slow reactivation phase observable in panels A and B, along with data from an experiment carried out at pH 5.9. Other experimental conditions were 45 °C, electrode rotation rate 2500 rpm. See Figure 3 for the route map followed, except for the reactivation potential which is now -233 mV. The dotted lines in panels A and B indicate the amount of film recovery expected from control experiments carried out without inactivating with O_2 . The dashed line indicates the current expected were 100% activity to be recovered after O_2 injection.

Table 1. Rate Constants for Activation of the Unready State of *A. vinosum* [NiFe]-Hydrogenase, at Different Temperatures, pH 6.0, under 1 bar H_2

T (°C)	k/s^{-1}
50	0.0038
45	0.0025
40	0.0016
35	0.0008
30	0.00047

slow phase. No difference in either the rate of reactivation or the proportion of fast phase to slow phase was observed.

Finally, experiments were conducted to establish (A) if Unready can be activated reductively without H_2 (i.e., using electrons alone), and (B) if not, whether CO can substitute for H_2 . Figure 12 shows the results of two experiments. Knowing the extent to which the Unready state is activated under H_2 after specific time periods, it was easy to introduce N_2 (instead of H_2) into the headspace for a fixed length of time, judged to be

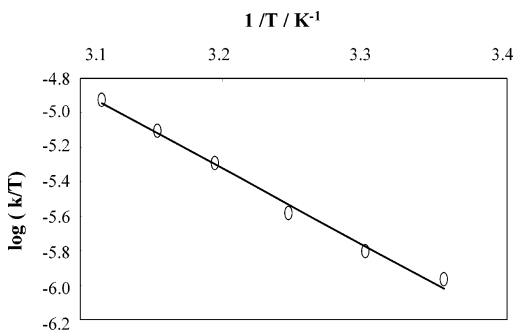


Figure 11. Temperature dependence of reductive activation of the Unready state of [NiFe]-hydrogenase. Plot of $\log(k/T)$ versus $1/T$ (Eyring plot) using data from chronoamperometric experiments at different temperatures. In all cases, the electrode potential was initially held at -558 mV before being stepped to 242 mV. After 60 s, 0.10 mL of O_2 -saturated buffer was injected, and then H_2 (1 bar) was passed through the headspace for 600 s, before stepping the potential back to -158 mV to initiate reactivation. From the data, $\Delta H = 84 \pm 0.7$ kJ mol $^{-1}$, and $\Delta S = -28 \pm 5$ J K mol $^{-1}$. Other experimental conditions: pH 6.0 and electrode rotation rate 2500 rpm.

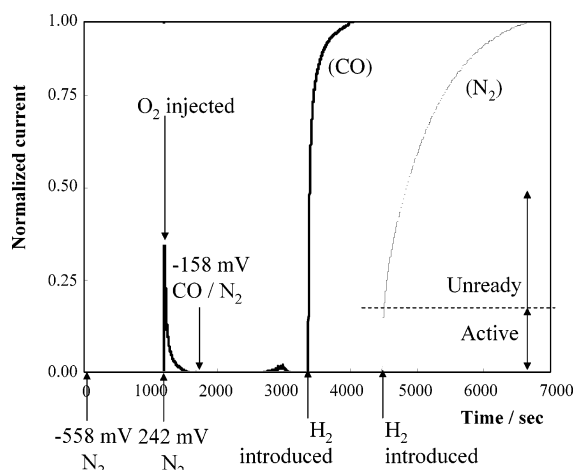


Figure 12. Chronoamperometry experiments to investigate the activation of the Unready state of [NiFe]-hydrogenase under N_2 and CO. The thin black line shows an experiment in which the enzyme has been held at -558 mV under N_2 for 600 s before the potential was stepped to 242 mV and 0.1 mL of O_2 -saturated buffer was injected (forming greater than 80% Unready). After the enzyme was flushed with N_2 for 600 s, the potential was stepped down to -78 mV, where it was held for 2700 s before H_2 was then introduced. Clearly, little of the enzyme has been activated during the period at low potential, as shown by the large amplitude of the slow phase. The thick black line shows an identical experiment except that CO was introduced after the potential step to -78 mV for 1200 s, followed by a short flush for 300 s with N_2 (to remove CO that is free in solution) before H_2 was introduced and the activity was monitored. The labeling and the terms “Active” and “Unready” correspond to the experiment carried out entirely under N_2 .

sufficient to observe full activation were the enzyme to be held under H_2 , then replace the N_2 by H_2 and measure how much enzyme has actually been activated. In this experiment, the enzyme was subjected to a potential of -78 mV under a N_2 atmosphere for 25 min, which is sufficient time to cause $>90\%$ activation under H_2 ; yet less than 20% was actually found to be active when H_2 was placed in the headspace. The remainder proceeded to activate at the same rate as observed (see above) when a low potential and H_2 were imposed simultaneously. (The rate of slow phase activation measured at -78 mV is slightly lower than that measured at -108 mV). Interestingly, when incubation included a period (20 min) under 1 bar CO, followed by 5 min under 1 bar N_2 , introduction of H_2 resulted in the

rapid recovery of 100% activity (without any slow phase) at a rate comparable to that observed in similar electrochemical experiments when H_2 replaces CO that has been added as an inhibitor.⁴³

Discussion

As demonstrated in Figure 2A, inactivation of *A. vinosum* [NiFe]-hydrogenase by exposure to O_2 is fast (trace i), in marked contrast to the slow inactivation (trace ii) that is induced under anaerobic conditions by holding the electrode at high potential.^{34,43,44} This is strong evidence that the oxidation process is inner-sphere; that is, it involves direct attack of O_2 at the NiFe center. Indeed, simple consideration of the kinetic diameters of H_2 (2.71 Å), O_2 (3.55 Å), and Xe (4.78 Å)³⁷ shows that O_2 can use the route taken by H_2 (note that Xe is used to study the H_2 channel using X-ray diffraction⁷). Remote outer-sphere electron transfer, as might instead occur at the distal [4Fe–4S] cluster (producing superoxide and ultimately peroxide), should give a slow rate similar to that observed at an electrode, where the reaction is probably limited by transport or binding of the hydrophilic species H_2O or OH^- to the active site.³⁴ The cyclic voltammogram (Figure 2B) shows that reductive reactivation of most of the enzyme molecules, previously subjected to an injection of O_2 while under H_2 , appears as a sharp peaklike response. The characteristic potential of the rise in activity (E_{switch} , obtained easily from the derivative di/dE and marked with a vertical bar) is close to the value observed after anaerobic inactivation and assigned to activation of the Ready state.³⁴ As discussed later, the conditions under which this experiment was carried out (injecting O_2 during turnover under H_2 while the electrode potential is still below 0 V) yield only a very small fraction of Unready state. It is important to note that recent stopped-flow FTIR studies have established that the reaction of H_2 -reduced enzyme with O_2 is complete within 0.2 s and results in the oxidized, Ready state Ni_i^* .⁴⁰

The formation of a second inactive species, displaying a much slower rate of reductive activation, is clearly evident from chronoamperometry experiments carried out over a wider range of conditions. Figure 3 shows that reductive reactivation of enzyme that has been inactivated by injecting O_2 during H_2 oxidation at 242 mV shows a fast phase lasting only seconds and a slow phase persisting for over 20 min. The slowly activating species is also observed in experiments in which proton reduction activity is measured (Figure 4), although the results are complicated – certainly by product inhibition at least (Figure 5). The biphasic behavior is in stark contrast to experiments carried out under entirely anaerobic conditions (applying an oxidizing potential without injecting O_2) in which the reductive reactivation shows only a single fast phase attributable to the Ready state.³⁴ Indeed, the rate of the fast phase is very potential dependent, as observed for the Ready state formed under anaerobic conditions.³⁴ The slow activation is fully consistent with the results reported by Albracht and others^{38,44–46} for the activation of Unready. At 45 °C, the half-life is approximately 5 min, but extrapolation of the activation data

(43) Lamle, S. E.; Vincent, K. A.; Halliwell, M. L.; Albracht, S. P. J.; Armstrong, F. A. *Dalton Trans.* **2003**, 4152–4157.

(44) Mege, R. M.; Bourdillon, C. *J. Biol. Chem.* **1985**, *260*, 14701–14706.

(45) Fernández, V. M.; Hatchikian, E. C.; Cammack, R. *Biochim. Biophys. Acta* **1985**, *832*, 69–79.

(46) Fernández, V. M.; Fernández, M. A.; Cammack, R. *Biochimie* **1986**, *68*, 43–48.

shown in Figure 11 shows that the rate at 20 °C would be 0.0002 s⁻¹, that is, a half-life of about 1 h for reductive activation. The rates are thus higher (but not significantly so) than comparable data reported for the enzyme from *D. gigas* (0.0004 s⁻¹, half-life approximately 30 min at 40 °C).^{10,25} We therefore conclude that the ratio of amplitudes of the slow and fast phase provides a convenient and reliable evaluation of the amount of either species formed under different conditions.

The results shown in Figure 6 show that injection of O₂ at high potential under a N₂ atmosphere favors formation of the Unready state, whereas injection of O₂ while the enzyme is under H₂ and held at more negative potentials produces a much higher proportion of the Ready state. Figure 7 shows that the amount of Unready formed under N₂ drops gradually as the potential is lowered, but even at 0 mV the fraction is still around 40%. Formation of the Unready state under H₂ is greatly enhanced when O₂ is injected at high potential, and the data shown in Figure 7 lie on a curve in which a negligible amount of Unready is formed below 100 mV. Unlike stoichiometric experiments in which a particular active state is preformed and then mixed with O₂,⁴⁰ the experiments described here address the reaction with O₂ that is initiated during turnover. Because the electrode potential and H₂ pressure each act to bias the steady-state oxidation level of the different centers in the active enzyme, it must be this factor, the availability of electrons, which determines whether reaction with O₂ leads to the Ready or Unready state.

As mentioned in the Introduction, the oxidation level of the enzyme is defined not only by the states of the NiFe center but also by the states of the Fe–S clusters. Extending the notation of Scheme 1, the two highest oxidation levels for the active enzyme are Ni_a–S(ooo) (with the [3Fe–4S] cluster oxidized) and Ni_a–S(oro) (with the [3Fe–4S] cluster reduced): these states can lose, respectively, only one or two electrons upon oxidation. The Ni_a–S(ooo) state is thermodynamically unstable because the [3Fe–4S]⁺⁰ potential is higher than the Ni(III)/Ni(II) potential, but a small fraction will be present under turnover conditions. By contrast, the lower oxidation states, including Ni_a–C* and Ni_a–SR and states with the distal and proximal clusters also reduced, can undergo multiple-electron oxidation. The electrode itself is a continuous and tunable source of electrons, and provided the [NiFe] center is active, any H₂ molecule contained in the enzyme's "gas channel" is also a potential electron donor. We therefore conclude that during H₂ oxidation, and provided the potential is not taken too high, all four electrons required to reduce O₂ completely will be available. By contrast, under N₂ and at high potential, there will probably not be enough electrons immediately available to reduce one molecule of O₂ to two molecules of H₂O.

At pH 8.8, under H₂, only about 20% of the enzyme that is inactivated by O₂ at high potential is produced in the Unready state, whereas on lowering the pH to 6.0 this percentage rises to approximately 40%. When inactivated under N₂, the difference is even more obvious, because at pH 8.8 the percentage of Unready is 40% as compared to 80% at pH 6.0. Thus, while pH does not affect the rate of activation of Unready, it has a large influence on its formation. Although our electrochemical experiments do not reveal the kinetics of reaction with O₂ because this is too fast, it is important to note that our electrochemical data are obtained under potential control, so

that the different behavior observed at pH 6.0 versus 8.8 is not a result of the change in the reducing power of an electron donor. It is interesting that formation of Ready is preferred when there are fewer protons available, despite the thermodynamic requirement for more protons. The pH effect is therefore kinetic in origin, the commitment to forming Unready or Ready depending on the protonation state of a species at some branching point on the reaction coordinate.

We now consider two options to account for the dependence of inactive product on electron availability. These are as follows: (Option A) The O₂ molecule is not fully reduced and the intermediate is trapped by the active site, resulting in the Unready state. (Option B) If there is a shortage of electrons when O₂ attacks, there is increased formation of an alternative conformation. The first of these options implies either that the bridging group in the Unready state is not a hydroxide ion, but an O–O species such as peroxide, or that if it is a hydroxide, an additional oxidizing species (such as an O-atom) is retained elsewhere. For example, an O-atom could transfer to one of the Ni-cysteine ligands, yielding a sulfoxide (>S=O)⁴⁷ or sulfenic acid (–S–OH) group.⁴⁸

The intriguing feature of the activation of Unready is that the rate is independent of electrode potential at values below E_{switch} . This behavior is very different from that observed for the Ready state, for which the rate of activation increases greatly with decreasing potential even at values more than 100 mV more negative than E_{switch} . These conclusions are unequivocal; the ability of the electrode to control the driving force is a powerful tool. Furthermore, there is no marked effect of pH or H/D solvent substitution on this rate. Recent studies by De Lacey et al.²⁵ have also shown that activation of the Unready state (using the *D. gigas* enzyme) shows no H/D isotope effect. These observations show that the rate-determining step is an inherent property of the enzyme rather than a factor that is directly related to the electrodriving force. While these qualifications initially appear more in line with Option B, a difference in conformation is very difficult to reconcile with the lack of equilibration between Unready and Ready states.

Focusing on Option A, we consider first the possibility that an intact, reduced O–O species is trapped as a ligand.⁴⁹ This would have to be a peroxide rather than a superoxide because the presence of the latter ($S = 1/2$) would be evident from the EPR spectrum. While the formation of a peroxide rather than superoxide appears inconsistent with the observation that Unready is formed by increasing the potential far above the reduction potential for the [3Fe–4S]⁺⁰ cluster, which helps to sustain the Ni_a–S(ooo) state with only one electron available to reduce O₂, this need not be the case when the enzyme is attached to an electrode. If a superoxide is initially formed by a reaction with Ni(II), and its reduction potential is high (free O₂⁻ has a potential of approximately 0.9 V),⁵⁰ the electrode

(47) Grapperhaus, C. A.; Darensbourg, M. Y. *Acc. Chem. Res.* **1998**, *31*, 451–459.

(48) Claiborne, A. L.; Mallett, T. C.; Yeh, J. I.; Luba, J.; Parsonage, D. *Adv. Protein Chem.* **2001**, *58*, 215–276.

(49) Recent X-ray structure studies support the assignment of a peroxide ligand in a bridging position in the Unready form of the [NiFe]-hydrogenase from *D. gigas* (Fontecilla-Camps, J. C., personal communication. Volbeda, A.; Martin, L.; Cavazza, C.; Matho, M.; Faber, B. W.; Roseboom, W.; Albracht, S. P. J.; Garcin, E.; Rousset, M.; Fontecilla-Camps, J. C., submitted).

(50) Bertini, I.; Gray, H. B.; Lippard, S. J.; Valentine, J. S. *Bioinorganic Chemistry*; University Science Books: Mill Valley, CA, 1994.

will provide electrons (via the enzyme's chain of Fe–S clusters) to reduce it rapidly to peroxide in a spontaneous and undetected process. The second possibility is that the additional oxidizing capacity on the Unready relative to the Ready state is equivalent to one oxygen atom that has transferred to a suitable acceptor within the active site. The obvious candidate is one of the non-bridging cysteine-S atoms, as these are well known to undergo oxygenation to a sulfoxide or to a sulfenic acid. In studies on small Ni(II) thiolate complexes, Darensbourg and co-workers have shown⁴⁷ that reaction with O₂ results in oxygenation of thiolate sulfur atoms to produce sulfoxides (>S=O) and sulfones (>S(=O)₂), either of which remain S-coordinated to Ni with surprisingly little effect on the Ni–S bonding. We believe that a sulfone (which could form without any prior reduction of enzyme) is unlikely as there is no evidence that fully oxidized enzyme (i.e., the Ready state) reacts with O₂ to form the Unready state. Alternatively, a sulfur could be oxygenated to give a sulfenic acid (–S–OH) or sulfenate, although this would probably change the mode of metal coordination.^{47,48} Both the peroxide and the sulfoxide/sulfenate possibilities are fully consistent with the observation that Unready and Ready are not in intrinsic equilibrium, because it is not energetically feasible to convert a hydroxide into a peroxide or an oxygenated-S. A third possibility is that both types of oxidized product are formed in parallel; however, the clean kinetics that we observe for the activation of Unready are more consistent with a single species, although the formation of an unreactive side-product, such as products of multiple oxygenation, may account for at least some of the unrecovered activity.

Some immediate questions remain. (a) Why is the trapped O-entity not rapidly reduced further? (b) Why is the formation of Unready favored at low pH? The fact that Unready (once established) does not take up further electrons even if these are made available suggests strongly that the O-species is a “dead-end” complex, the formation of which is due to electrons not having been available at some crucial stage of the pathway that otherwise leads to the Ready state and complete reduction of the attacking O₂. At this crucial stage, either an O²⁻ (or H₂O, HO⁻) is formed while the “hot” O-atom is trapped by a sulfur, or a peroxide is formed. Although peroxides are known as powerful oxidants, their reduction involves O–O cleavage and is not necessarily fast. In peroxidases, once peroxide is coordinated to Fe(III), it is important to be able to transfer a second proton onto the distal O-atom, which can then leave as H₂O while the other O-atom is stabilized as a high-valent Fe=O intermediate that is reduced in one-electron steps: peroxidase mutants that are unable to do this are inactive.⁵¹ Hence, it is by no means likely that reduction of peroxide can occur rapidly in this active site. The formation of Unready may therefore arise because, without a sufficient supply of electrons, a crucial mechanistic opportunity for proceeding directly to transfer of the third and fourth electrons is missed.

Our attention is now turning to the mechanism of activation of Unready. Most obviously, the only species that could escape without involving its reduction to water is peroxide. Reduction of Ni(III) should labilize a bound peroxide, and proton transfer to HOO⁻ would give H₂O₂ which is a better leaving group. The major difference might then be the relatively large size of

H₂O₂, making escape from the active site more difficult than for H₂O. In support of this possibility, the negative entropy of activation shows that the transition state is relatively ordered, thus suggesting that the O-species is still intact at this point. Alternatively, removal of an O-atom attached to a S-ligand would require two electrons to form water or hydroxide, which could then leave the active site. From model studies,⁴⁷ it appears that O-atom transfer between S-ligands is reversible in the presence of reductants; thus it is expected that O-atom removal will also require the reduction of Ni(III) to Ni(II). Finally, an important clue is provided by the results shown in Figure 12, which show that electrons alone are not sufficient to activate Unready, but that H₂ is required in the process. It is therefore highly significant that CO, which is well known as an inhibitor and likely to function only as a good π -acceptor ligand, is also an activator.⁵² This suggests that ligand displacement, in addition to reduction, is required. The mechanism of activation of Unready and the roles of H₂ and CO are now under close investigation.

Conclusions

In conclusion, protein film voltammetry experiments have allowed us to study in detail the potential dependences and kinetics of the aerobic interconversions of [NiFe]-hydrogenase and gain new insight into the properties of the Unready state (Ni–A/Ni_u*) that is formed upon contact with O₂. Of particular significance is the conclusion that Unready is formed under conditions that do not favor complete reduction of O₂ to two H₂O. The results lend significant support for a proposal in which Unready differs from Ready in having two extra oxidizing equivalents. These could be stored as a trapped O-atom (a sulfoxide (>S=O) or a sulfenic acid (S–OH)) or as a coordinated peroxo-ligand (as opposed to a hydroxo/oxo-ligand as has previously been assumed) and explains why Unready and Ready (Ni–A and Ni–B) do not interconvert freely. Not surprisingly, the activation of Unready proceeds by a mechanism that is very different from that for the activation of Ready; in particular, the rate, once corrected for thermodynamics, is remarkably independent of the electrodic driving force (the potential below E_{switch}), pH, and whether the solvent is H₂O versus D₂O.²⁵ The exact nature of this rate-determining step is now under investigation; in particular, it is important to establish the role that H₂ and CO may play in the activation process.⁵²

Acknowledgment. We thank the UK EPSRC, BBSRC (43/E16711), and The Netherlands Organization for Scientific Research (NWO) division for Chemical Science for funding. We are grateful to Dr. Kylie Vincent for her design of electrochemical apparatus, Dr. Winfried Roseboom for his help with enzyme preparation, and Drs. Anne Volbeda and Juan Fontecilla-Camps for helpful discussions.

JA047939V

(51) Bateman, L.; Léger, C.; Goodin, D. B.; Armstrong, F. A. *J. Am. Chem. Soc.* **2001**, *123*, 9260–9263.

(52) Evidence for an activating role for CO was reported in the 1980s, see: Berlier, Y. M.; Fauque, G. D.; LeGall, J.; Lespinat, P. A.; Peck, H. D., Jr. *FEBS Lett.* **1987**, *221*, 241–244.